LA-UR- 98-1975

Approved for public release; distribution is unlimited.

Title: Improvement of luminescent properties of thin-film phosphors by excimer laser processing

CONF-980447--

Author(s): J. McKittrick, C. F. Bacalski, G. A. Hirata
University of California at San Diego

R. C. Sze, J. Mourant, K. V. Salazar, and M. Trkula
Los Alamos National Laboratory

Submitted to: Proceedings of SPIE

Los Alamos
NATIONAL LABORATORY

DISCLAIMER

Improvement of luminescent properties of thin-film phosphors by excimer laser processing

J. McKittrick, C. F. Bacalski and G. A. Hirata
Dept. of Applied Mechanics and Engineering Sciences and Materials Science Program, University of California at San Diego, 9500 Gilman Drive, La Jolla, CA 92093-0411

R. C. Sze[a], J. Mourant[a], K. V. Salazar[b], and M. Trkula[b]
[a] Chemical Sciences and Technology Division
[b] Materials Science and Technology Division,
Los Alamos National Laboratory, Los Alamos, NM 87545

ABSTRACT

Thin-films of europium doped yttrium oxide, $(Y_{1-x}Eu_x)_2O_3$, were deposited on sapphire substrates by metallorganic chemical vapor deposition. The films, ~400 nm thick, were weakly luminescent in the as-deposited condition. A KrF laser was pulsed once on the surface of the films at a fluence level between 0.9-2.3 J/cm^2. One pulse was sufficient to melt the film, which increased the photoluminescent emission intensity. Melting of a rough surface resulted in smoothing of the surface. The highest energy pulse resulted in a decrease in luminous intensity, presumably due to material removal. Computational modeling of the laser melting and ablation process predicted that a significant fraction of the film is removed by ablation at the highest fluence levels.

Keywords: phosphors, luminescence, yttrium oxide, europium, laser melting, thin films

1. INTRODUCTION

Phosphors are inorganic solids that emit light when excited with an external energy source such as high energy photons, electrons or an electric field. Europium doped yttrium oxide $(Y_{1-x}Eu_x)_2O_3$, $x \leq 0.10$, is a well known photo- and cathodoluminescent phosphor used in the lighting industry and in cathode ray tube displays[1]. The material fluoresces a red/orange color (feature wavelength = 611 nm) when excited by high energy photons or electrons. The fluorescent emission results from the 5d→4f electronic transitions in the Eu^{3+} ion. Figure 1 shows the energy level diagram for the free Eu^{3+} ion. Since the rare earth elements in a solid are shielded by the outer 5s and 5p electrons, the free ion scheme can be used to analyze the transitions occurring in an ionic crystal. Excitation of the Eu^{3+} ion results in the promotion of the electrons into the ^5D_J manifold with emission occurring during relaxation to the ^7F_J ground state manifold.

Photo- and cathodoluminescent thin-films have potential application in emissive flat panel displays such as field emission and plasma panel displays. Field emission flat panel displays require thinner screens that operate under lower voltages, without sacrificing brightness or contrast. Thin-films, as opposed to the traditional discreet powder screens, offer the benefit of reduced light scattering, a reduction of material waste and the potential to fabricate smaller pixel sizes to enhance resolution. However, low temperature thin-film deposition techniques (e.g. sputtering, evaporation, chemical vapor deposition, laser ablation, etc.) typically produce amorphous or poorly crystalline films that require high temperature annealing to optimize the luminous efficiency. It is well documented that an increase in processing or post-synthesis annealing temperature increases the luminescent efficiency of $(Y_{1-x}Eu_x)_2O_3$ phosphors[2]. Unfortunately, these temperatures are higher than the

Further author information:
JM: Email: jmckittrick@ucsd.edu; Telephone: 619-534-5425; Fax: 619-534-5698
MT: Email: mtrkula@lanl.gov; Telephone: 505-667-0591; Fax: 505-667-8109

decomposition temperature of low cost glass (e.g. Corning 7059 which has a strain point of ~600°C), a desirable substrate from a manufacturing point of view. This is a major obstacle in utilizing thin-film phosphors in display applications.

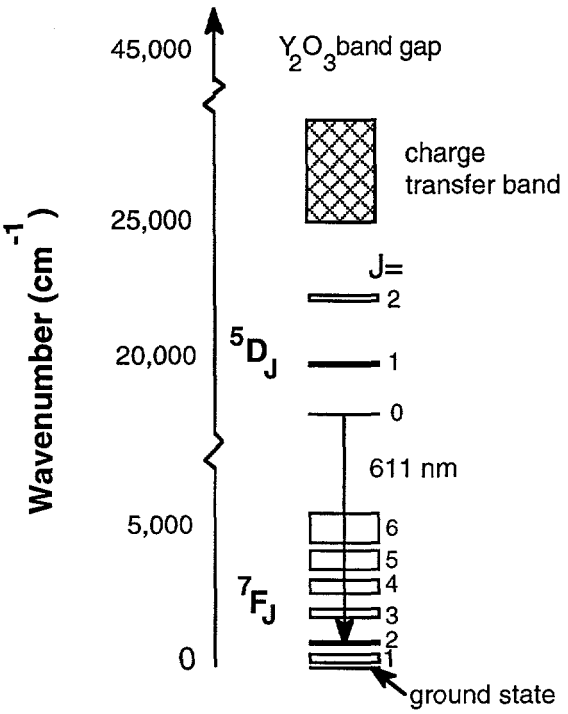

Figure 1 Partial energy level diagram for Eu^{3+} in Y_2O_3. The strong transition causing the 611 nm feature in the fluorescence spectra is shown. The charge transfer is the lowest level absorption band in this system with the band gap absorption occurring at a higher energy level. Adapted from reference 11.

When a high intensity ultraviolet (UV), pulsed photon beam is absorbed by the surface of a material, the transfer of energy produces a high local temperature. This can be used to melt and subsequently solidify the irradiated area and/or to simply alter the surface structure of the solid. Pulsed excimer lasers have been used to crystallize amorphous lead titanate films[3] and amorphous semiconductors[4-7], induce grain growth in silicon through melting and solidification[8], and to clean and smooth the surfaces of materials[9]. Thermal processing of thin-film phosphors by laser treatment has many advantages over standard heat treatment methods. The substrate is not exposed to elevated temperatures that can cause chemical reactions between the substrate and film or cause degradation of the substrate. The processing times and impurity diffusion are reduced and is an extremely fast clean process, free of heater elements and contaminants usually found in conventional furnaces. Moreover, the tendency in microelectronics fabrication is to reduce the number of processing steps. From this point of view, laser based techniques are attractive since they do not require sophisticated lithographic preparation of the wafers[10].

Thin-film $(Y_{1-x}Eu_x)_2O_3$ has been deposited by low pressure metallorganic chemical vapor deposition (MOCVD)[2,12-14], spray pyrolysis[15] and pulsed laser ablation[2,16-18]. Independent of the deposition technique, the as-synthesized films were found to be weakly luminescent and required post-deposition annealing to increase the emission intensity. The increase in luminescence was found to be related to the increase in crystallite size and/or crystal field strength[14]. Films containing smaller crystallites have more grain boundaries, which are thought to be non-luminescent or even luminescence quenching regions due to the disorder[19]. Thus, through melting and solidification of the material it may be possible to refine the grain

size and simultaneously improve the crystal field strength. Solidification studies of Y_2O_3-based phosphors have not been previously investigated due to the high melting point of Y_2O_3 (2420°C).

The objective of this work was to apply a high energy laser pulse onto the surface of an amorphous or weakly crystalline thin films of $(Y_{1-x}Eu_x)_2O_3$ to investigate if an improvement in the luminescent emission intensity could be achieved by laser melting or annealing.

2. EXPERIMENTAL PROCEDURES

$(Y_{1-x}Eu_x)_2O_3$ thin films were deposited by MOCVD with yttrium and europium tris(2,2,6,6,-tetramethyl-3,5-heptanedionates) precursors. The reaction chamber is a cold-wall, vertical design with a shower head for the precursor inlet. The shower head is 3 cm in diameter and contains an array of 3 mm circular holes. Inside the reaction chamber, sapphire substrates with the (001) face exposed were placed on the heater state 5 cm from the shower head inlet. The precursor reservoirs were heated to 146°C to sublime the organometallic species. Argon carrier gas passed through the heated reservoirs to transport the vapor to the reaction chamber. Oxygen gas was used as the oxidant during the growth process. Oxygen flowed into the chamber through two inlets positioned at ±60° to the substrates. During deposition the substrate temperature was maintained at temperatures between 500 or 600°C as monitored by a thermocouple. Mass flow controllers regulated the argon and oxygen flows separately. The total pressure inside the chamber was maintained with down stream control. Table I shows the deposition parameters.

After the deposition, the samples were allowed to cool to room temperature inside the chamber. Small scratches were made on the films with a diamond stylus and the film thickness was measured with a surface profilometer. Photoluminescence (PL) measurements were made on an Acton Research spectrograph with a UV Hg excitation source. A spot 2 mm in diameter was incident on the film and the emission spectra were collected in transmission mode with a 200 μm fiber optic cable. The as-deposited films were laser processed with a Lambda-Physik KrF excimer laser ($\lambda = 248$ nm) with a 25 ns pulse width. A homogenizer was used to produce a rectangular beam shape approximately 4 x 5 mm in size and a fluence between 0.9-2.3 J/cm^2. The laser treated films were subsequently analyzed by scanning electron microscopy (SEM) and PL spectroscopy. The thermal profile and melt and ablation depths were calculated by using a finite difference simulation program called SLIM, Simulation of Laser Interaction with Materials[20].

3. RESULTS AND DISCUSSION

The as-deposited films were weakly luminescent with the characteristic red/orange emission of $(Y_{1-x}Eu_x)_2O_3$ when excited by a UV hand lamp. Figure 1(a) shows the SEM micrograph of a ~400 nm thick film deposited at 500°C for six hours. The surface is very smooth and has a grain size of ~3 μm. Figure 1(b) shows the film after the application of one pulse at 0.9 J/cm^2. The micrograph shows there was some thermal cracking and melting is observed at the grain boundaries. Porosity has also been induced at the grain boundaries. This is presumably due to ablation as the ablation ejecta can be seen on the surface around the pores. As shown in Figure 1(c), after one pulse at 1.4 J/cm^2, a larger fraction of melting is observed. Because the grain boundaries are no longer seen, it appears that the whole surface melted. An increase in the amount of ablated material is also detected. After one pulse at 2.3 J/cm^2, the surface is considerably rougher than at the lower fluence levels and large solidification voids can be observed, as shown in Figure 1(d).

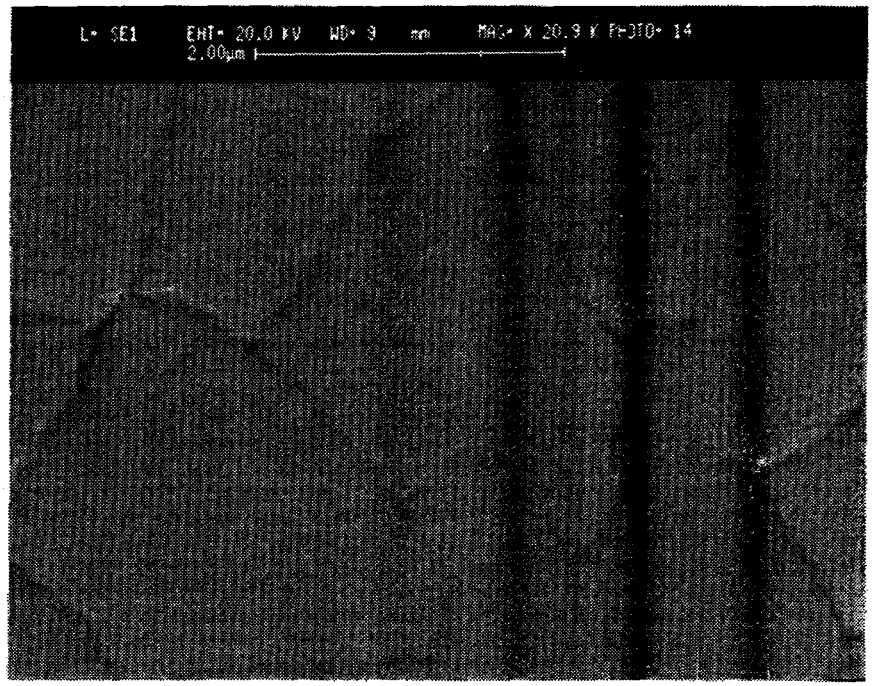

(a)

(b)

Figure 2 SEM micrograph of the (a) as-deposited $(Y_{1-x}Eu_x)_2O_3$, (b) after one pulse at 0.9 J/cm^2, (c) after one pulse at 1.4 J/cm^2, and (d) after one pulse at 2.3 J/cm^2.

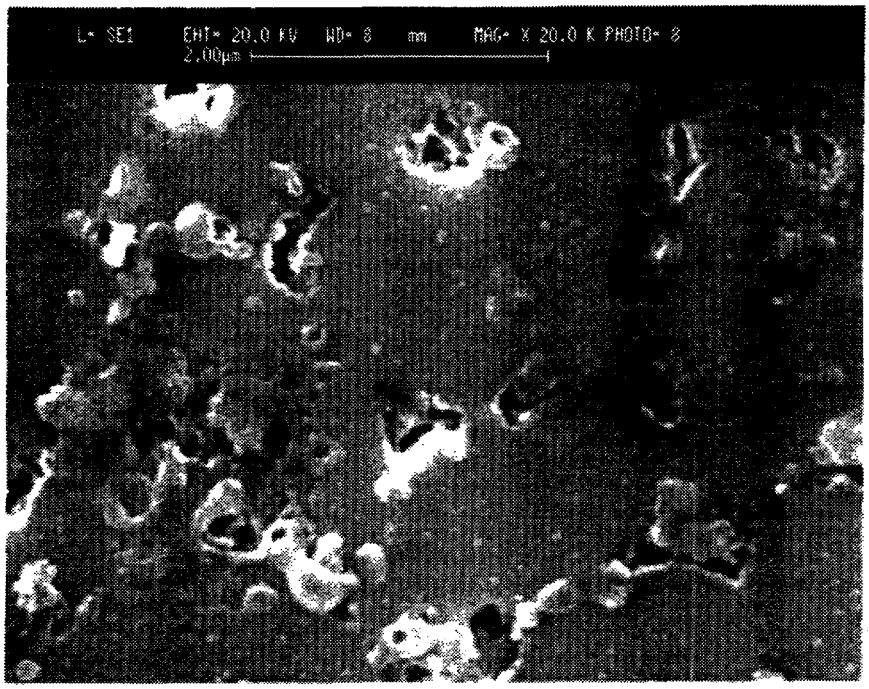

(c)

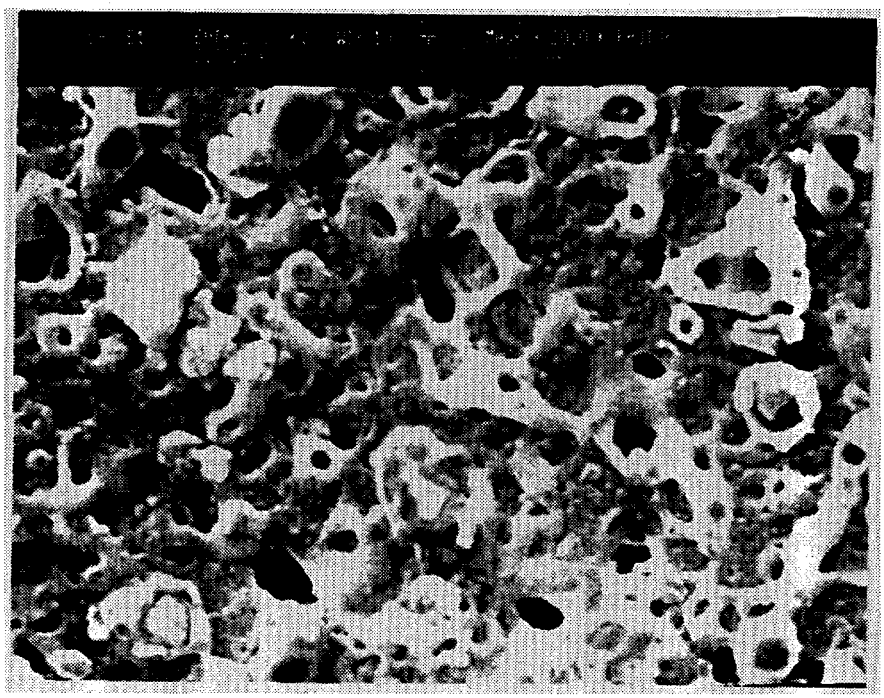

(d)

Figure 2 (cont.) SEM micrograph of the (a) as-deposited $(Y_{1-x}Eu_x)_2O_3$, (b) after one pulse at 0.9 J/cm^2, (c) after one pulse at 1.4 J/cm^2, and (d) after one pulse at 2.3 J/cm^2.

substrate	sapphire
substrate temperature	500 or 600°C
carrier gas	argon
metallorganic precursors	Y- or Eu-tris (2,2,6,6-tetramethyl-3,5-heptanedionate)
Y carrier gas flow rate	100 standard cm^3/min. (sccm)
Eu carrier gas flow rate	10 sccm
Y reservoir temperature	146°C
Eu reservoir temperature	146°C
oxygen gas flow rate	100 sccm
chamber pressure	5 Torr
deposition time	4 or 6 hours

Table I MOCVD deposition parameters.

Another experiment started with a different surface morphology, a film grown at 600°C for four hours with pronounced surface roughness and was laser processed at 1 J/cm^2. Figure 3(a) shows the SEM micrograph of the as-deposited film. The surface is composed of grains on the order of 3 μm with a roughness approximately on the same scale. After the application of one pulse of the laser, the surface was smoothed, as shown in the SEM micrograph in Figure 3(b). The porosity is on the order of 1-3 μm and is randomly distributed on the surface. It appears that the individual grains melted and solidified together and porosity resulted from the less than full density of the as-deposited MOCVD surface layer.

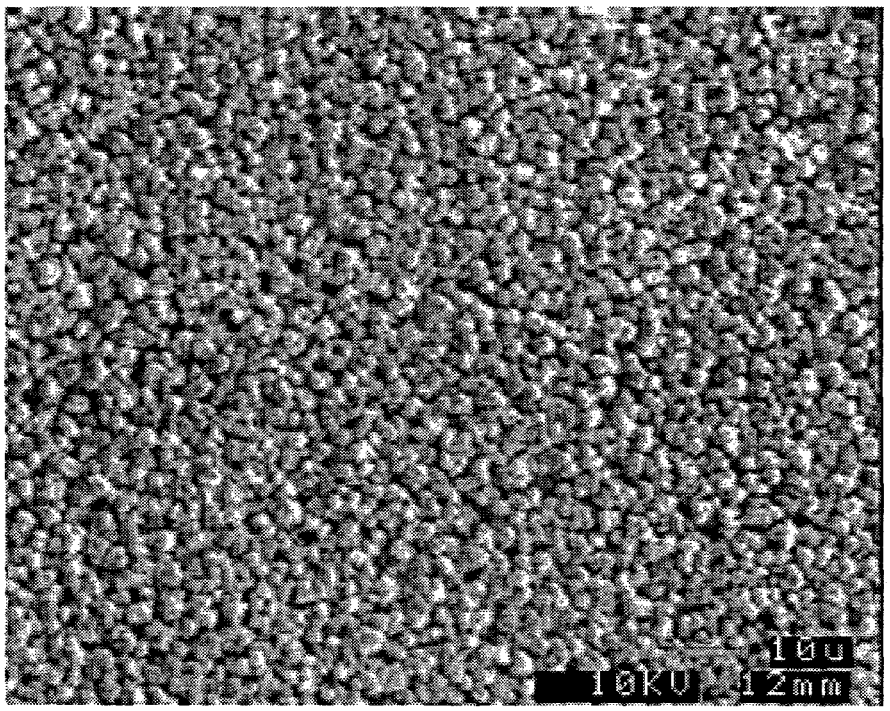

(a)

Figure 3 SEM micrograph of the (a) as-deposited $(Y_{1-x}Eu_x)_2O_3$ grown at 600°C for four hours, (b) after one pulse at 1.0 J/cm^2.

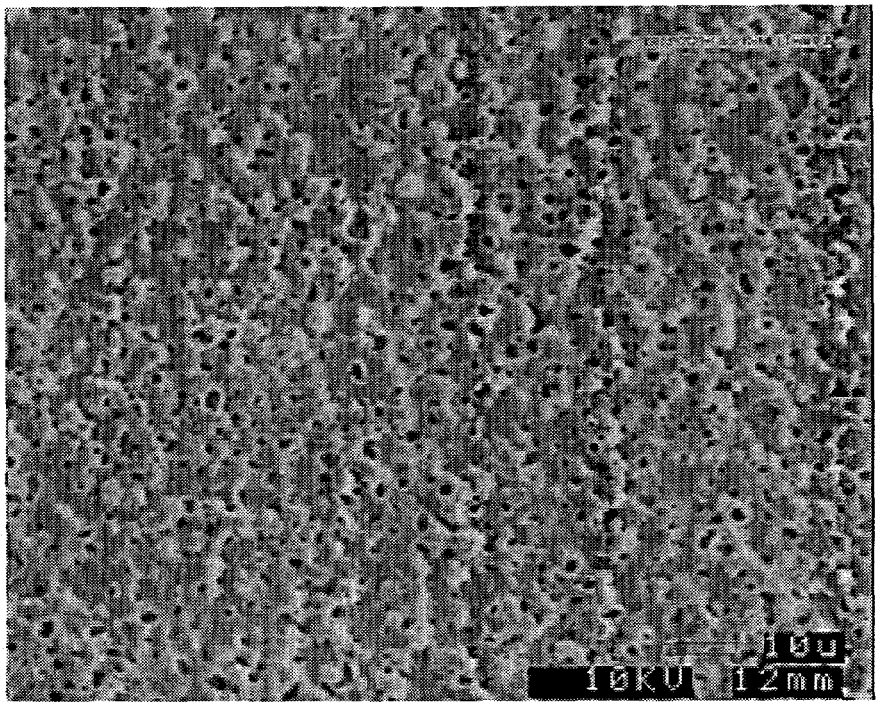

(b)

Figure 3 (cont.) SEM micrograph of the (a) as-deposited $(Y_{1-x}Eu_x)_2O_3$ grown at 600°C for four hours, (b) after one pulse at 1.0 J/cm^2.

PL measurements show the emission intensity of the laser processed film is greater than the as-deposited film. Figure 4 shows the PL emission spectra from 330-650 nm in which two distinct features are observed. The first is the transmission of the excitation source lines (404.7 and 435.6 nm). This feature is more intense in the as-deposited film, indicating that the laser processing densified the film, more fully absorbing and/or scattering the radiation. The second is the emission from the europium ion. The spectra show an increase in the integrated intensity of the laser processed film over that of the as-deposited film. It appears that melting and the subsequent solidification of the film can significantly improve the photoluminescence emission.

PL measurements on the films laser processed with different fluences is shown in Figure 5. The characteristic 611 nm feature of cubic $(Y_{1-x}Eu_x)_2O_3$ is seen along with the 628 nm feature identified with monoclinic $(Y_{1-x}Eu_x)_2O_3$ [21]. Monoclinic Y_2O_3 is a metastable phase, thought to be stabilized under ambient conditions by the Gibbs-Thompson effect as nanocrystalline particles. In the as-deposited state, the emission intensity is very weak, and the monoclinic feature is more intense than the one for the cubic structure. After the application of 0.9 J/cm^2, the emission intensity increased for both the cubic and monoclinic features. The highest emission intensity occurred for 1.4 J/cm^2, where the cubic feature is significantly higher than the monoclinic feature. An increase to 2.3 J/cm^2 decreased the emission intensity, which was unexpected.

Because of the decrease in PL emission intensity with increasing fluence, a computer simulation of the melting and ablation process as a function of time was performed with the SLIM program. The input data is given in Table II. The output of this program gives the surface temperature, the melt and ablation depths as a function of time and the thermal profile as a function of depth into the film. The simulations were run with a 400 nm $(Y_{1-x}Eu_x)_2O_3$ film on a semi-infinite Al_2O_3 substrate with a 500 ps time iteration interval with a square laser pulse with a fluence of 0.9, 1.4 or 2.3 J/cm^2.

Figure 6 shows the calculated results from the SLIM program. The melt depth (solid symbols) and ablation depth (open symbols) are shown as a function of time. A fluence of 0.9 J/cm^2 shows a melt depth maximum to be 280 nm. This

increases to 330 nm at 1.4 J/cm^2 and to 400 nm at 2.3 J/cm^2. This indicates that melting should have been observed for all the fluence levels used in this experiment, and is corroborated by the SEM micrographs. The decrease in PL intensity for the 2.3 J/cm^3 fluence can be correlated with the large ablation depth. For a fluence of 0.9 J/cm^2, there is no significant ablation. At 2.3 J/cm^2, an ablation depth of 160 nm was calculated, which is 40% of the original thickness of the film. The removal of this material can account for the decrease in PL intensity at this fluence level. Although it is expected that melting of the entire film would optimize the emission intensity, this fluence level removes too much of the material. Thus there needs to be a balance between maximizing the melt depth and minimizing the ablation depth to optimize the luminescent properties.

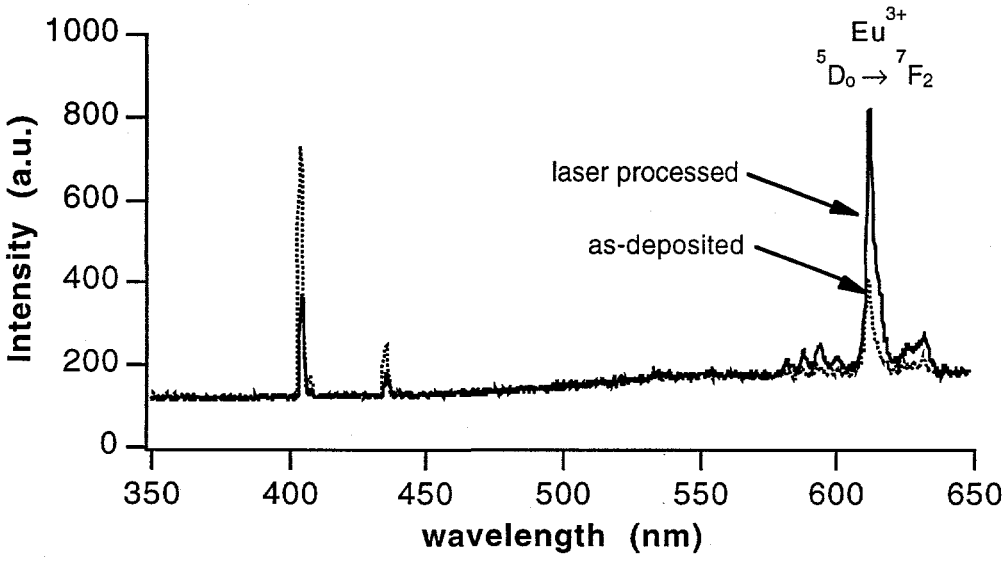

Figure 4 Photoluminescent emission spectra of the as-deposited and laser processed $Y_2O_3:Eu^{3+}$ thin-film. The Hg lines from the excitation source are visible at 404.7 and 435.6 nm.

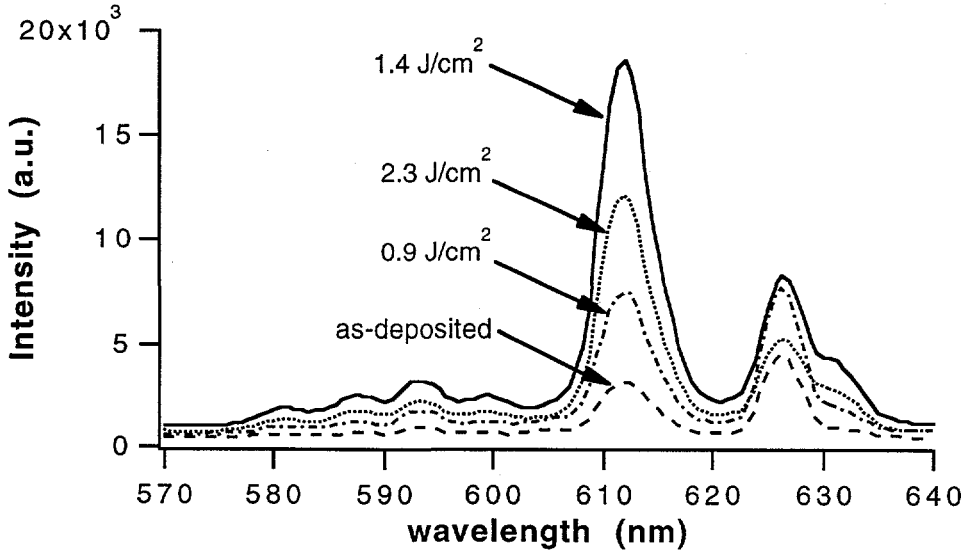

Figure 5 Photoluminescent emission spectra of the as-deposited and laser processed $(Y_{1-x}Eu_x)_2O_3$ thin-films.

Property	Al_2O_3 (substrate)	Y_2O_3 (film)
melting temperature (K)	2323	2693
evaporation temperature (K)	3253	4603
heat of melting (J/cm^3)	4400	2220
heat of vaporization (J/cm^3)	18,912	43,499
thermal conductivity (W/cm-K)		
solid	$48.6\ T^{-0.894}$	$6.86\ T^{-0.823}$
liquid	0.0476	0.0103
heat capacity (J/cm^3-K)		
solid	$7.15x10^{-4}\ T - 1.18x10^5T^{-2} + 4.26$	$7.29x10^{-4}\ T - 1.96x10^4T^{-2} + 2.31$
liquid	5.9	4.27
absorption coefficient (cm^{-1})		
solid	$5x10^4$	$5x10^4$
liquid	$5x10^4$	$5x10^4$
reflectivity (J/cm^3-K)		
solid		0.2
liquid		0.2

Table II Input parameters for the SLIM program. Data taken from reference 22.

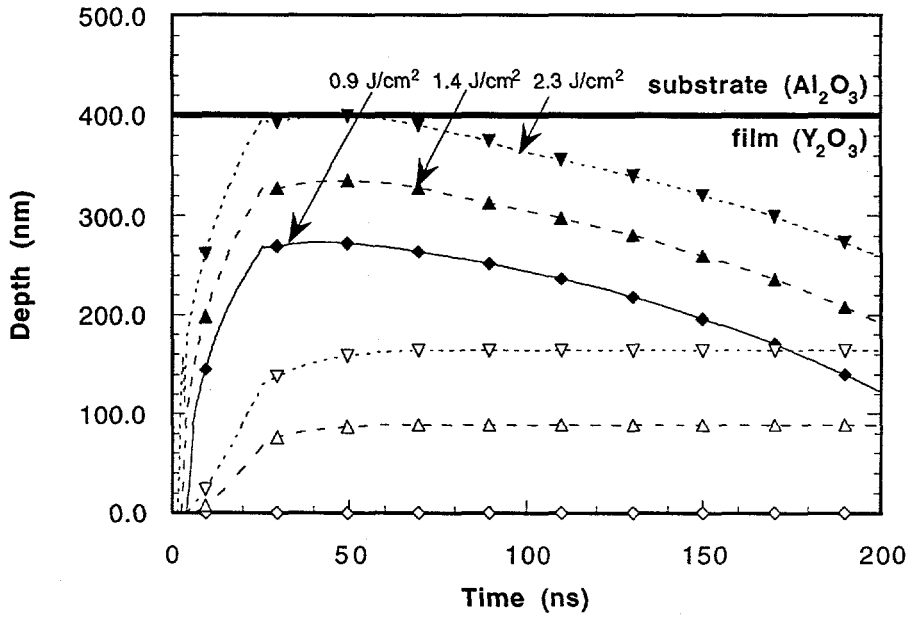

Figure 6 Calculated melt and ablation depth profiles by the SLIM program for different fluence levels. Solid symbols represent the melt depth, open symbols represent ablation depth.

4. CONCLUSIONS

Thin-film phosphors with a composition $(Y_{1-x}Eu_x)_2O_3$ were synthesized by chemical vapor deposition from organometallic precursors. Laser melting of the thin-film was achieved with a 248 nm KrF excimer laser with a pulse width of 25 ns and at fluences between 0.9-2.3 J/cm^2. The laser pulse melted the as-deposited film which increased the photoluminescent emission intensity. The photoluminescent emission intensity increased with higher fluence levels, however significant ablation occurred at the highest fluence level. Laser melting was also observed to smooth the surface of films with significant surface roughness. Computational modeling of the melt and ablation depth indicated that a significant portion of the film was ablated at the highest fluence level, which would decrease the photoluminescent emission intensity.

5. ACKNOWLEDGEMENTS

We would like to thank Ross Muenchausen at LANL for helping with the SLIM calculations. This work was conducted under the auspices of the US Department of Energy, supported (in part) by funds provided by the University of California for the conduct of discretionary research by Los Alamos National Laboratory under project CULAR and the Visiting Scholar Program and through the Phosphor Technology Center of Excellence by DARPA Grant No. MDA972-93-1-0030.

6. REFERENCES

1. K. A. Franz, W. G. Kehr, A. Siggel, J. Wieczoreck, in Ullmann's Encyclopedia of Industrial Chemistry, eds. B. Elvers, S. Hawkins, and G. Schulz, **A15**, VCH Publishers, Weinheim, Germany 1985.
2. G. A. Hirata, J. McKittrick, M. Avalos-Borja, J. M. Sisqueiros and D. Devlin, "Physical properties of Y_2O_3:Eu luminescent films grown by MOCVD and laser ablation," *Appl. Surf. Sci.*, **113/114**, 509 (1997).
3. J. S. Im, H. J. Kim and M. O. Thompson, "Phase transformation mechanisms involved in excimer laser crystallization of amorphous silicon films," *Appl. Phys. Lett.*, **63**, 1969 (1993).
4. P. M. Smith, S. Lombardo, M. J. Uttormark, S. J. Cook and M. O. Thompson, "Laser assisted e-beam epitaxial growth of Si/Ge alloys on Si," *Mater. Res. Soc. Symp. Proc.*, **202**, 603 (1991).
5. S. B. Xiong, Z. M. Ye, J. M. Liu, A.D. Li, C.-Y. Lin, S. Y. Chen, X. L. Guo and Z. G. Liu, "Crystallization of amorphous lead titanate thin films by the irradiation of KrF excimer laser," *Appl. Surf. Sci.*, **109/110**, 124-127 (1997).
6. C. N. Afonso, J. Solis, F. Vega, J. Siegel and W. Szyszko, "Solidification phenomena in Ge films upon nano- and pico-second laser pulse melting," *Appl. Surf. Sci.*, **109/110**, 20-24 (1997).
7. M. D. Efremov, V. V. Bolotov, V. A. Volodin, L. E. Fedina and E. A. Lipatnikov, "Excimer laser and rapid thermal annealing stimulation of solid-phase nucleation and crystallization in amorphous silicon films on glass substrates," *J. Phys.: Condens. Matter*, **8**, 273-286 (1996).
8. T. Sameshima, "Self organized grain growth larger than 1 μm through pulsed-laser-induced melting of silicon films," *Jpn. J. Appl. Phys.*, **32**, L1485-88 (1993).
9. V. N. Tokarev, W. Marine, C. Prat and M. Sentis, ""Clean" processing of polymers and smoothing of ceramics by pulsed laser melting," *J. Appl. Phys.*, **77** [9] 4714-23 (1995).
10. A. Desmur, B. Bourguignon, J. Boulmer, J. B. Ozenne, J. P. Budin, D. Debarre and A. Aliouchouche, "Pulsed laser etching of silicon: dopant profile modification and dopant desorption induced by surface melting," *J. Appl. Phys.*, **76**, 3081 (1994).
11. N. C. Chang, "Fluorescence and stimulated emission from trivalent europium in yttrium oxide," *J. Appl. Phys.*, **34** [12] 3500-3504 (1963).
12. J. P. Dismukes, J. Kane, B. Binggeli and H. P. Schweizer, "Chemical vapor deposition of cathodoluminescent phosphor layers," in Chemical Vapor Deposition: Fourth International Conference, eds. G.F. Wakefield and J.M. Blocher, The Electrochemical Society, Princeton, NJ, 1973.
13. G. A. West and K. W. Beeson, "Low-pressure metalorganic chemical vapor deposition of photoluminescent Eu-doped Y_2O_3 films," *J. Mater. Res.*, **5** [7] 1573-1580 (1990).

14. G. A. Hirata, J. McKittrick, J. Yi, S. G. Pattillo, K. V. Salazar and M. Trkula, "Microstructural and photoluminescence studies on europium doped yttrium oxide films synthesized by metallorganic vapor deposition," *Mat. Res. Soc. Symp. Proc.*, accepted.
15. H. P. Maruska, T. Parodos, N. M. Kalkhouraud and W. D. Halverson, "Challenges for Flat Panel Display Phosphors," *Mat. Res. Soc. Symp. Proc.*, **345** 269-280 (1994).
16. G. A. Hirata, J. McKittrick, M. Avalos-Borja, J. M. Sisqueiros and D. Devlin, "Physical properties of Y_2O_3:Eu luminescent films grown by MOCVD and laser ablation," *Appl. Surf. Sci.*, **113/114** 509-514 (1997).
17. K. G. Cho, D. Kumar, D. G. Lee, S. L. Jones, P. H. Holloway and R. K. Singh, "Improved luminescence properties of pulsed laser deposited Eu:Y_2O_3 thin films on diamond coated silicon substrates," *Appl. Phys. Lett.*, **71** [23] 3335-3337 (1997).
18. S. L. Jones, D. Kumar, R. K. Singh and P. H. Holloway, "Luminescence of pulsed laser deposited Eu doped yttrium Oxide films," *Appl. Phys. Lett.*, **71** [3] 404-406 (1997).
19. L. E. Shea, J. McKittrick and M. L. F. Phillips, "Predicting and modeling the low-voltage cathodoluminescent efficiency of oxide phosphors," *J. Electrochem. Soc.*, accepted.
20. SLIM, Simulation of Laser Interactions with Materials, R. Singh and J. Viatella, University of Florida, Gainesville, FL 32611-2066.
21. H. Eilers and B. M. Tissue, "Laser spectroscopy of nanocrystalline Eu_2O_3 and Eu^{3+}:Y_2O_3," *Chem. Phys. Lett.*, **251** 74-78 (1996).
22. G. V. Samsonov, The Oxide Handbook, translated from Russian by Robert K. Johnston, IFI/Plenum, New York, 1982.